Learning, Generalization, and Scalability of Abstract Myoelectric Control

Matthew Dyson, Sigrid Dupan, Hannah Jones, and Kianoush Nazarpour, *Senior Member, IEEE*

***Abstract*— Motor learning-based methods offer an alternative paradigm to machine learning-based methods for controlling upper-limb prosthetics. Within this paradigm, the patterns of muscular activity used for control can differ from those which control biological limbs. Practice expedites the learning of these new, functional patterns of muscular activity. We envisage that these methods can result in enhanced control without increasing device complexity. However, key questions about training protocols, generalisation and scalability of motor learning-based methods have remained. In this work, we pursue three objectives: 1) to validate the motor learning-based abstract myoelectric control approach with people with upper-limb difference for the first time; 2) to test whether, after training, participants can generalize their learning to tasks of increased difficulty; and 3) to show that abstract myoelectric control scales with additional input signals, offering a larger control range. In three experiments, 25 limb-intact participants and 8 people with a limb difference (congenital and acquired) experienced a motor learning-based myoelectric controlled interface. We show that participants with upper-limb difference can learn to control the interface and that performance increases with experience. Across experiments, participant performance on easier lower target density tasks generalized to more difficult higher target density tasks. A proof-of-concept study demonstrates that learning-based control scales with additional myoelectric channels. Our results show that human motor learning-based approaches can enhance the number of distinct outputs from the musculature, thereby increasing the functionality of prosthetic hands and providing a viable alternative to machine learning.**

***Index Terms*— Abstract decoding, myoelectric control.**

I. Introduction

THE most common method of controlling active hand prostheses is myoelectric control; use of the electromyogram (EMG) signals to estimate user intent [1]. Non-invasive EMG control has a number of attractive properties. For example, the EMG signal can be adapted to provide proportional control, the physical effort required resembles that of existing limbs, and the sensors systems are compact [2].

For users with trans-radial (below-elbow) limb difference, the "dual-site" control approach is commonly used. It provides bidirectional control of one degree of freedom (DoF) based on the EMG signals from a residual muscle pair. However, the functionality of the approach is limited due to the sequential nature of the control [3]. Targeted muscle reinnervation (TMR) provides a method whereby the number of independent muscle pairs for control may be increased, enabling the control of more DoF [4]. The current alternative to conventional prosthesis control is pattern recognition [5].

Pattern recognition prosthesis control typically aims to decode motor commands such that an intended movement maps to its prosthetic substitute. When using surface EMG, the intentions to be detected are usually limited to commonly used grasps [6], [7]. During calibration, said systems require EMG data representative of each grasp to train a classifier, which then categorizes new samples during actual use. Literature suggests that when a classifier is trained for each desired output, pattern recognition provides a viable method of prosthesis control [8]. This approach has recently reached the market [9], [10]. The core challenges which limit the robustness of pattern recognition control relate to ensuring training data adequately characterizes real world data [11].

Learning-based methods, which rely upon closed-loop feedback to adapt muscle behavior, have generated significant interest as a potential alternative approach for myoelectric prosthesis control [12]–[18]. Insight into the clinical readiness of such an approach has recently been provided [19]. A common component linking many of these methods is the presentation of muscle activity as feedback in a non-representational multidimensional space, such as a centre-out task, within which users must learn to control their muscle activity. The driving hypothesis is that once the skill is acquired in the non-representational space, arbitrary mappings may be made to functional outputs, such as proportional control of prosthetic digits [13] or selection of hand postures [17]. Because these methods are characteristically non-biomimetic, we refer to the approach as "abstract decoding" [18].

Presenting continuous feedback of muscle activity in a multidimensional space allows the motor system to generate an inverse map [20]. Inverse maps link motor output to

Manuscript received March 2, 2020; revised May 11, 2020 and May 21, 2020; accepted May 26, 2020. Date of publication June 5, 2020; date of current version July 8, 2020. This work was supported by the EPSRC under Grant EP/N023080/1 and Grant EP/R004242/1. *(Corresponding author: Kianoush Nazarpour.)*

Matthew Dyson, Sigrid Dupan, and Hannah Jones are with the School of Engineering, Newcastle University, Newcastle upon Tyne NE1 7RU, U.K. (e-mail: matthew.dyson@newcastle.ac.uk; sigrid.dupan@newcastle.ac.uk; hannah.jones@newcastle.ac.uk).

Kianoush Nazarpour is with the School of Engineering, Newcastle University, Newcastle upon Tyne NE1 7RU, U.K., and also with the Biosciences Research Institute, Newcastle University, Newcastle upon Tyne NE2 4HH, U.K. (e-mail: kianoush.nazarpour@newcastle.ac.uk).

This article has supplementary downloadable material available at http://ieeexplore.ieee.org, provided by the authors.

Digital Object Identifier 10.1109/TNSRE.2020.3000310

arbitrary control variables and multiple maps can be formed for different task spaces [21], [22]. Inverse maps allow generalization to untrained locations in the task space, making them distinct from associative learning which only allows retention of trained activity [20], [23]. Within a task space, errors in direction and gain are processed separately [24] and newly learned inverse maps can be adapted to compensate for spatial alterations [25]. When scaling errors generalize, gain adaptation of feed-forward control is rapid [24]. For clarity, we refer to this as *within-task* generalization to avoid confusion with *between-task* generalization, in which practice transfers to distinct activities [26].

In this paper, we present results from three complementary myoelectric control experiments. The first investigates how training influences performance and skill transfer. This experiment is intended to validate that our myoelectric control protocol generates inverse maps, rather than being based on associative learning [20], [23]. Validation is necessary because the underlying theory is based on studies of physical movement [20], [24], [25] and has not been explicitly addressed in the EMG domain [12]–[18]. The second experiment shows, for the first time, that participants with upper-limb difference can learn to operate the myoelectric interface with an abstract controller. This study extends results previously published in limb-intact participants [18], [27] under two control conditions: 1) direct, untransformed EMG signals and 2) spatially-weighted EMGs. The third study demonstrates that learning based control scales with additional EMG channels and can replicate results associated with state-of-the-art machine learning-based methods, without computational complexity.

II. Methods

A. Ethics

All participants gave informed written consent. Approval was granted by the local ethics committee at Newcastle University (Ref: 17-NAZ-056) and by Health Research Authority, UK (Ref: 16/SW/0347).

B. General Setup

Each of the experiments presented are very similar in nature. In all experiments, participants control a circular cursor on a computer screen with their muscle activity, that is a biofeedback setting. To avoid repetition, general properties shared across more than one experiment are outlined here.

1) Estimation of Muscle Activity: All muscle activity was smoothed using a mean absolute value (MAV) filter calculated over the preceding 750 ms window of the EMG signal. This window size has been found to balance the task requirements of responsive effector movement with sufficient stability during constant muscle contraction [13], [18]. Muscle activity used to control the cursor was updated at a variable rate, which exceeded and was asynchronous to the refresh rate of the display. At each task update step an acquisition thread was polled and any new samples available were added to the EMG window. This approach was used to ensure changes in EMG activation were reflected in cursor activity in the shortest possible time frame. In the following sections y refers to estimated muscle activity.

2) Calibration: A calibration routine was performed before each experiment. The primary purpose of calibration was to normalize muscle activation estimates. Operators observed EMG activity while participants performed muscle contractions. Contractions corresponded to wrist flexion and extension in limb-intact participants. In limb-deficient participants contractions corresponded to flexion and extension of the phantom wrist when appropriate. In other cases, pairs of muscles were selected based on independence of control. Participants were instructed to restrict muscle activity to that which could be maintained easily and repeated without risk of fatigue. In previous studies these prompts have produced EMG activity ranging between 10% to 20% of the maximum voluntary contraction [16], [27], [28]. Such a low muscle contraction level limits the signal-dependent noise [29] in the EMG signals, allowing for smoother control.

Data representative of baseline rest, y_r, and comfortable contraction, y_c were obtained for each EMG control channel. A vertical bar was presented to the participant. The height of the vertical bar corresponded to the real-time normalized muscle activation level, $\hat{y} = (y - y_r)/(y_c - y_r)$. Participants were instructed to briefly maintain the vertical bar at a fixed position for each muscle in order to ensure relative independence of activity. The normalized muscle activation level, $\hat{y}$, was used during experiments.

C. General Protocol

Experiment 1 and 2 used the myoelectric-controlled interface (MCI) described in [27]. The same protocol is briefly described here for completeness. For discussion of how the MCI relates to prosthesis control, please see our previous work.

Participants operated the MCI by performing isometric muscle contractions. Activity estimated from the contraction of two independent muscles determined the position of a 2-D circular cursor, as indicated in Fig. 1a. We use independent muscles to refer to any muscle pair which can be contracted in *relative* isolation to one another. Figure 1a shows a four target interface. The grey dashed line in Fig. 1a indicates where four targets would be subdivided to produce an eight target interface. In experiment 1, in addition to four and eight targets, in two runs, twelve targets were required. To achieve that, each of the four original targets were split into three zones along its length, making a 3-by-4 matrix of targets.

All muscle activity was normalized such that estimation, $\hat{y} = 1$, would bring the cursor to the top limit of the interface on the corresponding dimension. All trials commenced with the presentation of the cursor and the basket area at the origin of the interface which delimits little to no muscle activity. Participants had to be relaxed, such that the cursor remained within the basket, for the trial to commence. A target was presented when the trial started. A sample cursor trajectory from the basket to a target is shown in Fig. 1b.

Each trial was 1.5 seconds long and composed of two 750 ms segments - the move period and the hold period. The

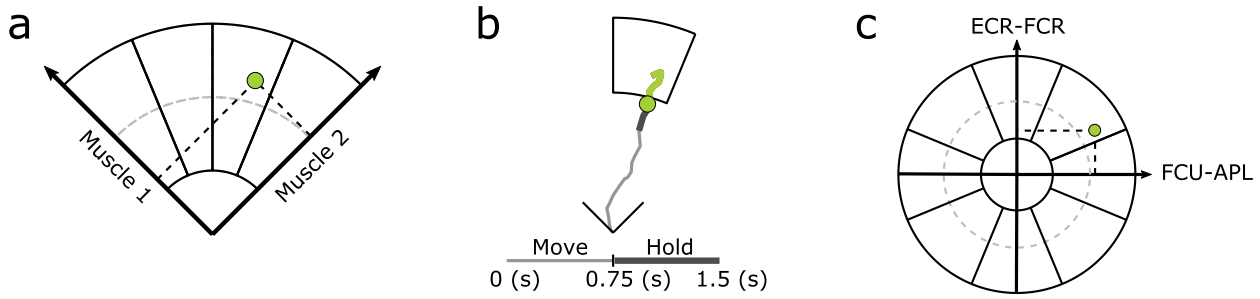

Fig. 1. Interfaces and trial timing protocols. (a) The standard 2-dimensional myoelectric interface control space. Participants used co-contraction of a muscle pair to move the cursor to targets. In Experiment 2, spatially-weighted muscle activity controlled the cursor position within the two axes. The grey dashed line indicates where four targets would be subdivided to produce an eight target interface. The same approach was adopted to create twelve targets. (b) A representative cursor trajectory in the task space. Thin and thick traces show trajectories during movement and hold periods respectively. Green indicates where cursor is in contact with or within the target to score ~70%. (c) The 4-channel interface used in Experiment 3 as a proof of concept. Cursor position on each axis was determined by the relative output of each muscle. ECR denotes extensor carpi radialis, FCU flexor carpi ulnaris, FCR flexor carpi radialis and APL abductor pollicis longus.

move period allowed time for reacting to presentation of the target and moving the cursor to the target. Participants were informed of the trial breakdown and were instructed to attempt to maximize their score by keeping the cursor within the target during the hold period. Trial score was calculated based on the amount of time the cursor spent within, or in contact with, the target during the hold period. The trial score was presented to the participant after each trial.

D. Analyses

In all experiments the primary metric used to define performance was trial score, as presented to the participant after each trial. Hit score refers to the percentage of trials in which the target was reached.

Performance in the larger participant population tended to be normally distributed, however at individual run level some data appeared multimodal. Normality of distributions was not assumed in the smaller amputee population. For consistency all comparisons were made using non-parametric statistical methods.

E. Experiment 1: Influence of Training Protocol

Experiment 1 was performed in order to ensure that the use of a structured training protocol, in which the number of targets increased progressively, produced the same results as a training protocol with higher accuracy demands from the onset.

Participants: Twenty-four limb-intact participants took part in this experiment (19 male and 5 female; age 22.17 $\pm$ 2.68). All were able-bodied and right–handed with no neurological disorders. Data from one participant was discarded due to lack of engagement. A replacement participant was recruited.

Recordings: Participants were seated in an experimental chair with their right hand in a pronated open position within a glove. The palm and fingers of the glove were adhered to a horizontal board attached to the armrest of the chair. A strap was placed over the lower wrist to restrain participants from lifting the forearm. The position of the board on which the glove was mounted was adjustable to ensure comfortable support for each participant's arm and hand.

Surface EMG signals were recorded from two forearm muscles: flexor carpi radialis (FCR) and extensor carpi radialis (ECR). Measurements were made using disposable snap electrodes (Bio-logic®, Natus Medical Inc., USA). Signals were amplified with a 5k gain (D360, Digitimer, UK), band-pass filtered (30 Hz–1 kHz) and sampled at 5 kHz (NI USB-6212 BNC, National Instruments, USA). The computations necessary to realize the experiment were performed on a desktop computer (3.2 GHz i5-3470 CPU, 8 GB RAM, Viglen Ltd, UK). Visual feedback was presented on a 17" LCD flat panel display (Belinea 101727, Germany) positioned approximately 1m in front of the participant.

Data were visually inspected for artefacts. Trials containing significant electrical noise, movement artefacts or any other traces which appeared to be non-physiological, were rejected. Mean artefact rejection rate across participants was 0.06% with a standard deviation of 0.14%.

Protocol: All participants initially completed a short run using a 12-target interface to assess baseline performance, as shown in Fig. 2b. Twelve targets were presented without repetition. The median score achieved over the 12 targets was used as the participants' baseline performance. After completing the run, each participant was assigned to one of two groups. Assignment was based on a moving average of the groups, i.e. participants were assigned such that the difference in mean baseline performance between the groups, at the time of test, was minimized, as shown in Fig. 2a. To create a reference for the moving average, participants 1-4 were assigned to the 8-8 group, while participants 5-8 were assigned to 4-8 group. Participants assigned to group one became the 8-8 group, those assigned to group two became the 4-8 group.

Participants operated the MCI over eight runs. Each run comprised 80 trials. The 8-8 group performed 8-target trials in all eight runs. The 4-8 group performed 4 runs of 4-target trials, followed by 4 runs of 8-target trials. A final run was used to test the generalization of the two training protocols. This run consisted of 72 trials using a 12-target interface. Figure 2b shows the number of targets presented in each of the ten experimental runs for both the 8-8 and the 4-8 group.

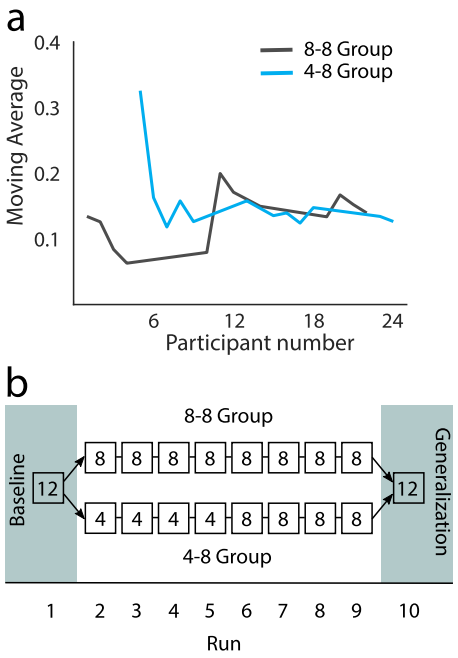

Fig. 2. Protocol information for Experiment 1. (a) Participant assignment to experimental group based on baseline performance and resulting group average baselines. Participants 1 to 4 were assigned to the 8-8 group, and participants 5 to 8 to the 4-8 group. Subsequent participants were assigned such that the difference in the moving average between the two groups was minimized. (b) Run number and target trial types for each experimental group. All participants perform a 12 target baseline performance run. Participants are assigned to the 8-8 group or 4-8 group, experiencing associated target types. All participants perform a 12 target assessment of generalization run.

F. Experiment 2: Validation With People With Upper-Limb Difference

In Experiment 2, participants learned to use the MCI using the training approach validated in Experiment 1. Participants controlled the MCI under two conditions: using two untransformed EMG signals and using spatial weighting of multiple EMGs. Use of two untransformed signals is of comparable technical complexity to the current clinical standard for upper-limb myoelectric control. Spatial weighting of EMG can detect ensemble activities, sometimes termed muscle synergies, and is closer to the standard used in pattern recognition systems.

Participants: Eight participants took part in this experiment. Six participants had trans-radial limb deficiency and two participants had trans-humeral limb deficiency. Both the trans-radial and trans-humeral groups were equally balanced between congenital and acquired cases. One trans-radial participant had a left limb deficiency, all remaining participants had right limb deficiencies. Two of the trans-radial participants use myoelectric prosthesis (Bebionic hand) proficiently, with the dual-site controller. Further participants details can be found in Table I.

Recordings: Participants sat in a lever operated office chair with optional arm support and were free to move their residual limb during experiments. Visual feedback of the task was provided by a 24" LED flat panel display (Hanns.G, Taipei, Taiwan), placed approximately 1m in front of the participant.

TABLE I
EXPERIMENT 2: PARTICIPANT INFORMATION DETAILS. TABLE SHOWS PARTICIPANT GENDER (M: MALE, F: FEMALE) AND AGE; TYPE (TR: TRANS-RADIAL, TH: TRANS-HUMERAL), CAUSE AND SIDE OF LIMB-LOSS (L: LEFT, R RIGHT); NUMBER OF YEARS WITH LIMB DIFFERENCE AND ANY PROSTHESIS USE

Participant	Gender	Age	Type	Cause	Side	Years	Prosthesis use
1	M	54	TR	Illness	R	18	None
2	F	25	TH	Congenital	L	25	None
3	M	28	TR	Accident	R	6	Split hook
4	F	30	TH	Accident	L	3	None
5	M	55	TR	Congenital	L	55	Myoelectric
6	F	40	TR	Congenital	R	40	None
7	M	55	TR	Accident	R	13	Myoelectric
8	F	50	TR	Congenital	R	50	None

Surface EMG signals were recorded using a Trigno Wireless EMG System and Trigno Acc parallel-bar EMG sensors (Delsys Inc. Natick, MA, USA).

In general, eight sensors were placed on the residual limb. In the case of one participant for whom eight sensors could not be accommodated on the residual limb, only four sensors were used. In cases where independent muscles could be manually distinguished in the residual limb, sensors were placed over the belly of the muscle. Where biological landmarks could be used to distinguish FCR and ECR in trans-radial participants, the muscle pair was selected. When FCR and or ECR could not be ascertained with certainty, independent muscles were first identified using manual handling and confirmed by inspection of raw EMG traces. After placing sensors over a minimum of two discernible independent muscles, the remaining sensors were spatially distributed around the residual limb. Signals were acquired at 2000 Hz and band-pass filtered between 20 Hz and 450 Hz. All subsequent computation necessary to realize the experiment were performed on a laptop computer (2.3 GHz i5-6200U CPU, 8 GB RAM, Lenovo, China).

Estimation of muscle activity: In addition to single channel data, muscle activity was estimated using spatial filters based on multiple sensors. Spatial weighting was performed using principal components analysis (PCA). Data for generating PCA weights were obtained during the calibration routine.

Calibration: When calibrating for EMG based control, two channels were selected based on participants' ability to independently control the available candidates. Calibration then followed the general routine described in the methods section. When calibrating for PCA based control, multi-channel data representative of the muscle activity required for cursor control were initially acquired. When FCR and ECR had been found using biological landmarks muscle activity would map to flexion and extension of the phantom wrist. In other cases, muscle activity appropriate for producing those contractions identified by manual handling and inspection of EMG traces were used. During data acquisition both participants and operators observed multi-channel EMG traces (time-series) in order to ensure the muscle contractions performed produced distinct activity in the sensor space. PCA weights were calculated using said multi-channel data. After calculation of PCA weights, calibration followed the routine used for EMG

TABLE II
EXPERIMENT 2: RECORDED RUNS FOR EACH PARTICIPANT. EMG REFERS TO USE OF TWO EMG CHANNELS FOR CURSOR CONTROL. PCA REFERS TO USE OF SPATIALLY WEIGHTED EMG CHANNELS FOR CURSOR CONTROL, WITH WEIGHTS OBTAINED USING PRINCIPAL COMPONENT ANALYSIS. 4 TARGET AND 8 TARGET INDICATE THE TARGET DENSITY OF THE INTERFACE

	EMG		PCA	
Participant	4 Target	8 Target	4 Target	8 Target
1	7	2	4	2
2	7		5	
3	11	19	4	4
4	4	4	4	4
5	4		4	
6	10	4	4	4
7	4	1		
8	4	4	4	4

based control; with two principal components being selected based on participants' ability to independently control the candidates available. In the PCA-based control, activity from two principal components, representing the weighted activity of eight sensors, determined the cursor position.

Protocol: All participants began using a 4-target interface. The number of runs performed using a 4-target interface was dependent on individual participant's ability, however all participants performed a minimum of four runs. When both operators and participants were satisfied that participants were ready, participants progressed to an 8-target interface, as shown in Fig. 1a. Both 4-target and 8-target runs comprised 48 trials. Due to the challenging nature of the protocol, progression was based on mutual decision rather than a fixed performance metric to ensure engagement and to minimize the risk of fatigue. Two muscle activation estimation methods were compared - use of individual surface EMG sensors and spatially-filtered EMG using PCA. Due to variability in participant performance and task progression being based on demonstrated ability, it was not feasible to systematically balance exposure to the EMG and PCA based control conditions. Participants performed the task at variable rates and over a differing number of days. All participants who used PCA based control also used EMG control on the same day in at least one session. Full details of the number of runs recorded for each participant are listed in Table II.

G. Experiment 3: Scalability

In Experiment 3, we increased the number of control sites and expanded the interface. We refer to these expansions as scalability because we aim to demonstrate how, after extensive practice, the performance patterns observed in participants using a simple interface hold when task and control complexity is scaled up.

Participants: As a proof of concept, one limb-intact right handed participant took part in this experiment. This participant was proficient in abstract myoelectric control.

Recordings: Surface EMG signals were acquired using a Trigno Wireless EMG System and Trigno IM parallel-bar EMG sensors. Four sensors were placed on the right forearm targeting, extensor carpi radialis (ECR), flexor carpi radialis (FCR), abductor pollicis longus (APL) and flexor carpi ulnaris (FCU). The experiment was performed on a laptop computer (2.1 GHz i7-4600U CPU, 8 GB RAM, Lenovo, China). All other aspects of data acquisition followed those detailed for Experiment 2.

Calibration: Calibration followed the standard routine extended to four channels. Care was taken to ensure muscle contractions could be performed to activate each muscle independently.

Protocol: The interface used in Experiment 3 expanded upon that already presented by including the remaining three quadrants necessary to create a generic centre-out task space. Muscles were mapped to the interface space in a manner which was intuitive for a hand held in a pronated position. Muscles ECR and FCR acted as an antagonistic pair mapped to up and down respectively. APL and FCU performed the same role for cursor movement to the left and right. This design was inspired by the task in [30]. As in the previous interface normalized muscle activity, $\hat{y} \approx 1$, would move the cursor to the limit of the interface on a given dimension. Cursor control was implemented as simply as possible. With an interface space mapped from -1 to 1 on both dimensions, vertical cursor position was determined by $\hat{y}_{ECR} - \hat{y}_{FCR}$ and horizontal position by $\hat{y}_{FCU} - \hat{y}_{APL}$. For clarity, an interface with 16 targets is shown in Fig 1c. Sections can be merged or further sub-divided to change the density of the targets.

The participant started using a centre-out 8-target interface. A minimum of four runs were performed before the option was given to progress onto the next size of target interface. Interfaces with 8, 16 and 24 targets were tested. All runs were performed over four sessions. The first two sessions and the final two sessions were separated by five months.

III. RESULTS

Results are presented in two areas of learning and generalization, which share common ground between the first two experiments, namely, 1) the influence of training paradigm and learning over runs; and 2) generalization of ability with increasing target density. Our final experiment demonstrates that both learning over runs and generalization of ability are applicable as the number of EMG control sites and target density increase. This serves as support for the scalability of the abstract decoding method.

A. Learning

Limb-intact participants controlled a myoelectric interface in Experiment 1. After an initial baseline testing with a myoelectric interface of 12-targets, they were assigned to one of two conditions: 1) 4-8, in which they operated a 4-target interface first and then moved to an 8-target interface in the later runs; and 2) 8-8, in which they only experienced an 8-target interface. Both groups performed a short run of 12-targets at the end. In Experiment 2, limb-deficient participants operated the interface with two of the eight EMG signals recorded from their remnant limb; or with two principal components of their muscle activity,

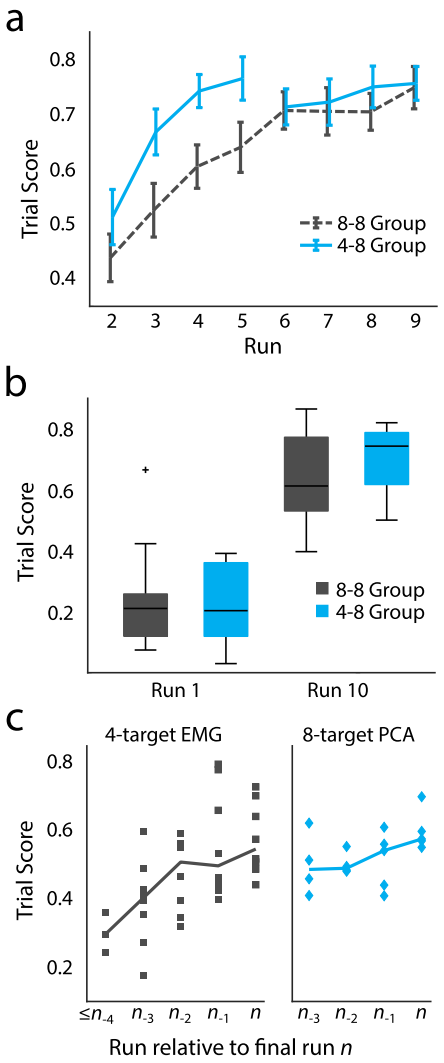

Fig. 3. Effect of learning over runs in terms of trial scores. (a) Experiment 1: mean and standard error of mean for participants over runs two to nine in the 8-8 group and the 4-8 group. (b) Experiment 1: box plots showing participant performance in run 1, the baseline assessment, and run 10, the generalization assessment, for the 8-8 group and the 4-8 group. (c) Experiment 2: median and individual participant results for 4-target EMG control and 8-target PCA based control, runs shown relative to final run using the same axes for trial score.

extracted from the eight EMG channels. In both experiments, participants sought to maximize trial score, the degree to which a cursor representing muscle activity reached a series of rapidly presented targets.

Fig. 3a-b show the effect of learning on myoelectric control over runs in Experiment 1. There was no difference in initial baseline performance between the 4-8 group (median: $Mdn = 0.21$) and the 8-8 group ($Mdn = 0.203$) (Wilcoxon rank sum, $Z = -0.0866$, $n1 = n2 = 12$, $p = 0.935$ two-tailed). Additionally, we found no effect of training protocol on participant performance, as evidenced by comparisons of performance on runs six and ten. For run six, the first in which both groups used an 8-target interface, no significant difference was found between the 8-8 group ($Mdn = 0.697$) and the 4-8 group ($Mdn = 0.742$) (Wilcoxon rank sum, $Z = -0.1443$, $n1 = n2 = 12$, $p = 0.885$ two-tailed).

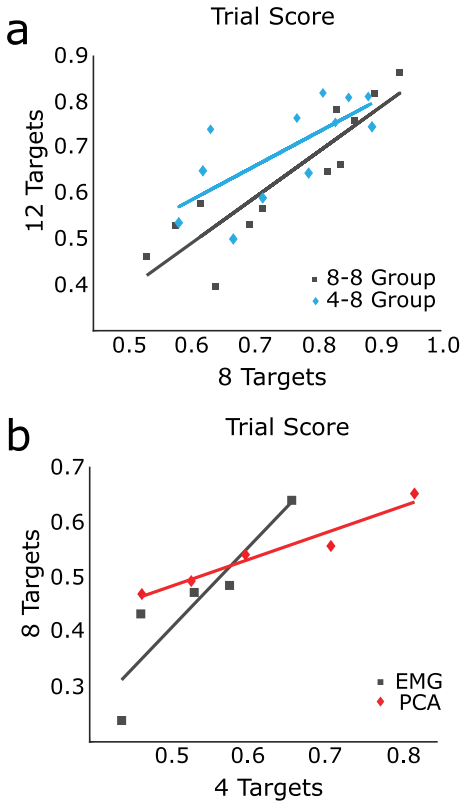

Fig. 4. Generalization of performance with increasing numbers of targets. (a) Experiment 1: participant performance on 8 targets relative to 12 targets for the 8-8 group and the 4-8 group. (b) Experiment 2: participant performance on 4 targets relative to 8 targets for both EMG and PCA based control.

Likewise, run ten, in which both groups used a twelve target interface, produced no significant difference in participant performance between the 8-8 group ($Mdn = 0.612$) and the 4-8 group ($Mdn = 0.743$) (Wilcoxon rank sum, $Z = -0.9526$, $n1 = n2 = 12$, $p = 0.341$ two-tailed). Performance on run ten, the generalization run, was significantly higher ($Mdn = 0.657$) than run one, the baseline assessment run, ($Mdn = 0.211$) (Wilcoxon signed-rank, $Z = -4.29$, $n = 24$, $p < 1e-04$). Figure 3c shows the effect of learning in limb-deficient participants over runs in Experiment 2. Note that final run performance in limb-deficient participants using the 8-target interface falls within the first and second quartiles of performance achieved in limb-intact participants.

In both Experiments 1 and 2, improvement in cursor control, as measured by hit score, preceded improved trial score. Hit scores were significantly related to trial score in all conditions, both across runs: Experiment 1 ($r = 0.988$, $p < 1e-05$, $n = 8$), Experiment 2 EMG ($r = 0.979$, $p < 0.05$, $n = 4$), Experiment 2 PCA ($r = 0.986$, $p < 0.05$, $n = 4$); and also across participants as measured in experimental final runs: experiment 1 ($r = 0.652$, $p < 1e-03$, $n = 24$), experiment 2 EMG ($r = 0.876$, $p < 0.01$, $n = 4$), experiment 2 PCA ($r = 0.812$, $p < 0.05$, $n = 4$).

B. Generalization

Participants' within-task generalization of performance across target layouts of increasing density are shown in Fig. 4.

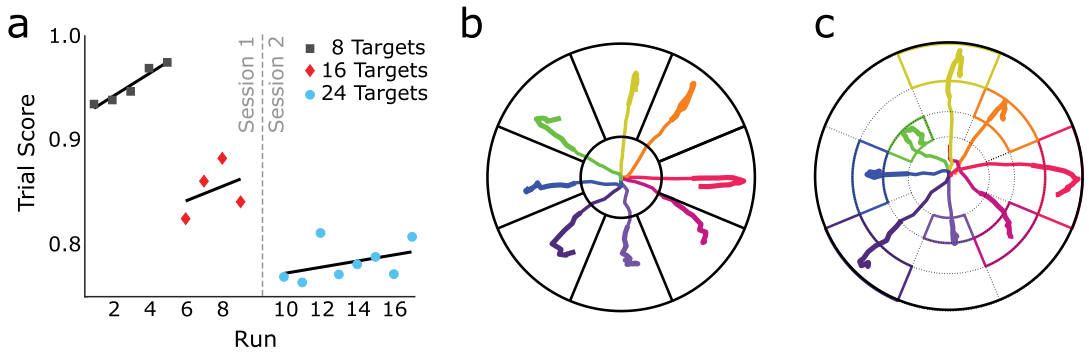

Fig. 5. The scalability of abstract decoding. (a) Participant performance progressing from use of an 8-target interface to a 24-target interface. Points show performance on individual runs which are displayed old to new on the horizontal axis. Dashed grey line indicates performance over different days. Lines of best fit are shown for performance on each interface size. (b) Representative cursor traces using an 8-target interface (c) Representative cursor traces using a 24-target interface.

In both Experiment 1 and Experiment 2, and across participant groups, individual participant performance using a simple target layout was predictive of their ability to generalize to one of increased complexity. In Experiment 1 there was significant correlation between participants' performance on their final 8-target run and their post-training performance in the 12-target run, for both the 8-8 group ($r = 0.896$, $n = 12$, $p < 1e{-}04$) and the 4-8 group ($r = 0.714$, $n = 12$, $p < 0.01$). In Experiment 2, significant correlations were found between final run performances on a 4-target interface and final run performance on an 8-target interface using control based on both EMG ($r = 0.911$, $n = 5$, $p < 0.05$) and principal components ($r = 0.971$, $n = 5$, $p < 0.01$).

C. Scalability

Individual participant performance while learning to use a centre-out task space is shown in Fig. 1c. Points in Fig. 5a show performance on individual runs. Markers differentiate between using an 8-, 16- and 24-target interface. Lines of best fit are included for each target density group and show a general trend of improvement in overall score for each target density over runs. Representative cursor trajectories during use of an 8-target interface and a 24-target interface are shown in Figures 5b and 5c. Data in Fig. 5 was obtained during the first two of four recording sessions. Session 2 was recorded three days after Session 1. Long-term retention of ability was probed in Sessions 3 and 4, which are presented in the supplementary material.

IV. Discussion

Neuroscience has been fascinated with how people learn motor tasks for decades [31], [32]. Studies of motor learning often depend upon modifying well established mappings through visual rotations [24] or perturbation [31]–[33] because it is difficult to create novel movements in physical space [20]. Human machine interfaces, including myoelectric control, are novel by default and have therefore acted as a catalyst to study how novel motor tasks are learned [12], [16], [23], [34]–[39]. Evidence suggests new mappings can be generated from scratch [20] and they can be arbitrary and non-intuitive [12], [15], although they do not have to be [17], [39], [40].

The experiments presented in this paper demonstrate that participants, both limb-intact and limb-deficient, can learn to control an 8-target myoelectric interface using muscles of the arm. Experiment 1 showed that the training protocol had no influence on eventual performance, rather performance increased based on the amount of runs completed. This observation was confirmed in Experiment 2. In addition, we showed for the first time that people with limb difference can learn to operate a myoelectric interface with an abstract decoder. In both Experiments 1 and 2, we found that once an inverse map of the task is learned with practice, within-task generalization to control spaces with more targets is possible. Our final experiment showed how abstract control can scale to higher target densities than required for rehabilitation.

Cursor control in our interface relies upon two factors: the relative magnitude of activity between muscles and their overall amplitude. In both task spaces in this paper, these parameters map to direction and extent respectively. If these variables are encoded independently, changes to one attribute should not influence the other. Previous research has shown that direction and extent can be learned and adapted independently [24], however the mapping from control to task space may influence whether this is the case [25].

As literature on gain generalization is inconclusive [24], [25], Experiment 1 was designed to determine whether the learning of gain control would generalize within our myoelectric interface space. Independence of direction and extent would imply that people can first learn a control space with less constrained scaling requirements, introducing a gradation of difficulty in order to maintain engagement [41]. We observed that participants who initially learned using the 4-target interface performed equivalently on an 8-target interface to those who learned on said 8-target interface. Our results show that gain generalizes within our control space. It may be the case that exploratory behaviour on the 4-target interface that did not contribute to task performance, i.e. exploring the space within targets influenced the generalization of gain. As this experiment was designed to inform our applied rehabilitation work with amputees using the same interface, we could not control for this confounding variable.

In Experiment 2, participants with limb-loss learned the same control scheme based on the structured training approach

validated in Experiment 1. This experiment confirmed that amputee participants' scores increased as they used the MCI. Within participants, performance using higher density target interfaces was correlated to overall score obtained when using lower density target interfaces. These observations are in line with the results of Experiment 1 and our earlier work with limb-intact participants [18]. Besides, we have previously shown that participants can perform this task without visual feedback, and that overall performance is predictive of the no feedback condition [18]. These, combined with the presented generalization results, support the working hypothesis that this task can be used to train users for prosthesis control.

Our third experiment illustrated that this method can translate to additional control sites and targets. The results of Experiment 3 largely corroborate the findings of previous learning-based myoelectric interfaces that utilized the centre-out task [12]–[15], [17], [19]. These experiments demonstrate that simultaneous proportional control with multiple muscles can be achieved without the use of statistical learning algorithms. Centre-out style control can be realized in a shorter time-frame through the use of classification [42] or regression [42]–[44] algorithms which weight multiple control sites based on calibration or training data. These algorithms allow immediate control, however little is known about how they influence longer term user adaptation and learning [45], [46].

In an upper-limb prosthetics context, the term *user-adaptation* is more common than user *learning*. It is essential to note the qualitative differences between this work and that of Hahne *et al.* [42], [44]. Aside from the fact that we use no regressors or classifiers, in the adaptation work of Hahne *et al.* [42], [44], participants experience relatively long periods of feedback in each trial (10 s). In contrast, we present very short trials which encourage reaching the target very quickly. Our parameters are selected to promote use of forward model, rather than use of visual feedback and within-trial adaptation. In this context, while online feedback may intervene [47] within-trial adaptation is not a viable control strategy and does not explain performance without visual feedback and changes to reaction times [18] nor retention of ability over sessions, as shown in Fig. 5a. For additional retention and reaction time data supporting our position, the reader is pointed to the supplementary material.

We do not anticipate retention of skills to differ between limb-deficient and limb-intact participants. Anecdotally, we observed that learning is often slower in amputee participants, however this is not consistent. Two factors, muscle fatigue and performance pressure, are likely to contribute to this difference. Currently, these types of human factors are the main limitation of this approach, rather than technical engineering challenges. As presented, our method relies on participants maintaining concentration, with an often delayed reward, for relatively long periods. Since it is probable that training will always be comparatively lengthy, we are developing gamified protocols to target user engagement. A corresponding technical challenge will be to validate that learned skills actually transfer to prosthesis control [48]. We do not view the work presented as controller implementations per se, rather as a framework within which arbitrary multidimensional spaces can be adapted according to the availability of control channels. For details of how the interface used in Experiment 1 and 2 was originally envisaged see [49]. We assume the method demonstrated in Experiment 3 could be used similarly to other centre out control schemes [13]–[15], [17], [19].

Exactly how to efficiently exploit learning in a human-machine interfacing context remains an open question [22]. Few papers directly address learning in a traditional prosthetics context [26], [46]. Nevertheless, prosthetics literature contains error-rates fit with exponential functions, characteristic of a typical learning curve, during extended use of both differential control [50] and pattern recognition [51]. Similarly, a form of learning was posited to significantly improve pattern recognition control in TMR patients during a long term home trial. Critically, no equivalent effect was found when using direct control [5]. While the general properties of myoelectric learning remain understudied, confounds will exist for machine learning-based approaches. This is particularly the case for long-term studies where the properties of the EMG signal change over time [46], [51]. When implementing adaptive or co-adaptive approaches that interact with changes, distinguishing user adaptation from machine learning will require even more complex controls [47].

We demonstrated that learning-based myoelectric approaches are a viable option for people with upper-limb difference. It also extends existing evidence demonstrating that such techniques can produce more nuanced myoelectric control than typically associated with prosthesis control. By replicating a typical myoelectric control task, we have shown how the method that we presented can scale with additional control sites. In replicating a task normally achieved using regression or classification we hope to draw attention to the role human learning may play in prosthesis control.

REFERENCES

[1] G. Hefftner and G. G. Jaros, "The electromyogram (EMG) as a control signal for functional neuromuscular stimulation. II. Practical demonstration of the EMG signature discrimination system," *IEEE Trans. Biomed. Eng.*, vol. 35, no. 4, pp. 238–242, Apr. 1988.

[2] P. Parker, K. Englehart, and B. Hudgins, "Myoelectric signal processing for control of powered limb prostheses," *J. Electromyogr. Kinesiol.*, vol. 16, no. 6, pp. 541–548, Dec. 2006.

[3] A. Muzumdar, *Powered Upper Limb Prostheses: Control, Implementation and Clinical Application*, 1st ed. Berlin, Germany: Springer, 2004.

[4] T. A. Kuiken, G. A. Dumanian, R. D. Lipschutz, L. A. Miller, and K. A. Stubblefield, "The use of targeted muscle reinnervation for improved myoelectric prosthesis control in a bilateral shoulder disarticulation amputee," *Prosthetics Orthotics Int.*, vol. 28, no. 3, pp. 245–253, Dec. 2004.

[5] L. J. Hargrove, L. A. Miller, K. Turner, and T. A. Kuiken, "Myoelectric pattern recognition outperforms direct control for transhumeral amputees with targeted muscle reinnervation: A randomized clinical trial," *Sci. Rep.*, vol. 7, no. 1, Dec. 2017, Art. no. 13840.

[6] B. Hudgins, P. Parker, and R. N. Scott, "A new strategy for multifunction myoelectric control," *IEEE Trans. Biomed. Eng.*, vol. 40, no. 1, pp. 82–94, 1993.

[7] K. Englehart and B. Hudgins, "A robust, real-time control scheme for multifunction myoelectric control," *IEEE Trans. Biomed. Eng.*, vol. 50, no. 7, pp. 848–854, Jul. 2003.

[8] M. Ortiz-Catalan, B. Hkansson, and R. Brnemark, "Real-time and simultaneous control of artificial limbs based on pattern recognition algorithms," *IEEE Trans. Neural Syst. Rehabil. Eng.*, vol. 22, no. 4, pp. 756–764, Jul. 2014.

[9] L. Coapt. (2019). *Coapt Engineering*. Accessed: Aug. 27, 2019. [Online]. Available: https://coaptengineering.com

[10] G. Ottobock. (2019). *Myo Plus Pattern Recognition*. Accessed: Aug. 27, 2019. [Online]. Available: https://www.ottobock.co.uk/prosthetics/upper-limb-prosthetics/product-systems/myo-plus/

[11] E. Scheme and K. Englehart, "Electromyogram pattern recognition for control of powered upper-limb prostheses: State of the art and challenges for clinical use," *J Rehabil. Res. Develop.*, vol. 48, no. 6, pp. 643–660, 2011.

[12] S. M. Radhakrishnan, S. N. Baker, and A. Jackson, "Learning a novel myoelectric-controlled interface task," *J. Neurophysiol.*, vol. 100, no. 4, pp. 2397–2408, Oct. 2008.

[13] T. Pistohl, C. Cipriani, A. Jackson, and K. Nazarpour, "Abstract and proportional myoelectric control for multi-fingered hand prostheses," *Ann. Biomed. Eng.*, vol. 41, no. 12, pp. 2687–2698, Dec. 2013.

[14] C. W. Antuvan, M. Ison, and P. Artemiadis, "Embedded human control of robots using myoelectric interfaces," *IEEE Trans. Neural Syst. Rehabil. Eng.*, vol. 22, no. 4, pp. 820–827, Jul. 2014.

[15] M. Ison and P. Artemiadis, "Proportional myoelectric control of robots: Muscle synergy development drives performance enhancement, retainment, and generalization," *IEEE Trans. Robot.*, vol. 31, no. 2, pp. 259–268, Apr. 2015.

[16] T. Pistohl, D. Joshi, G. Ganesh, A. Jackson, and K. Nazarpour, "Artificial proprioceptive feedback for myoelectric control," *IEEE Trans. Neural Syst. Rehabil. Eng.*, vol. 23, no. 3, pp. 498–507, May 2015.

[17] J. L. Segil and R. F. Weir, "Novel postural control algorithm for control of multifunctional myoelectric prosthetic hands," *J. Rehabil. Res. Develop.*, vol. 52, no. 4, pp. 449–466, 2015.

[18] M. Dyson, J. Barnes, and K. Nazarpour, "Myoelectric control with abstract decoders," *J. Neural Eng.*, vol. 15, no. 5, Oct. 2018, Art. no. 056003.

[19] J. L. Segil, R. Kaliki, J. Uellendahl, and R. F. F. Weir, "A myoelectric postural control algorithm for persons with transradial amputations: A consideration of clinical readiness," *IEEE Robot. Autom. Mag.*, vol. 27, no. 1, pp. 77–86, Mar. 2020.

[20] X. Liu and R. A. Scheidt, "Contributions of online visual feedback to the learning and generalization of novel finger coordination patterns," *J. Neurophysiol.*, vol. 99, no. 5, pp. 2546–2557, May 2008.

[21] D. M. Wolpert and M. Kawato, "Multiple paired forward and inverse models for motor control," *Neural Netw.*, vol. 11, nos. 7–8, pp. 1317–1329, Oct. 1998.

[22] F. A. Mussa-Ivaldi, M. Casadio, Z. C. Danziger, K. M. Mosier, and R. A. Scheidt, "Sensory motor remapping of space in human-machine interfaces," *Prog. Brain Res.*, vol. 191, pp. 45–64, 2011.

[23] K. M. Mosier, R. A. Scheidt, S. Acosta, and F. A. Mussa-Ivaldi, "Remapping hand movements in a novel geometrical environment," *J. Neurophysiol.*, vol. 94, no. 6, pp. 4362–4372, Dec. 2005.

[24] J. W. Krakauer, Z. M. Pine, M.-F. Ghilardi, and C. Ghez, "Learning of visuomotor transformations for vectorial planning of reaching trajectories," *J. Neurosci.*, vol. 20, no. 23, pp. 8916–8924, Dec. 2000.

[25] X. Liu, K. M. Mosier, F. A. Mussa-Ivaldi, M. Casadio, and R. A. Scheidt, "Reorganization of finger coordination patterns during adaptation to rotation and scaling of a newly learned sensorimotor transformation," *J. Neurophysiology*, vol. 105, no. 1, pp. 454–473, Jan. 2011.

[26] H. Bouwsema, C. K. van der Sluis, and R. M. Bongers, "Changes in performance over time while learning to use a myoelectric prosthesis," *J. NeuroEng. Rehabil.*, vol. 11, no. 1, p. 16, 2014.

[27] M. Dyson and K. Nazarpour, "Data driven spatial filtering can enhance abstract myoelectric control in amputees," in *Proc. 40th Annu. Int. Conf. IEEE Eng. Med. Biol. Soc. (EMBC)*, Jul. 2018, pp. 3770–3773.

[28] K. Nazarpour, A. Barnard, and A. Jackson, "Flexible cortical control of task-specific muscle synergies," *J. Neurosci.*, vol. 32, no. 36, pp. 12349–12360, Sep. 2012.

[29] C. M. Harris and D. M. Wolpert, "Signal-dependent noise determines motor planning," *Nature*, vol. 394, no. 6695, pp. 780–784, Aug. 1998.

[30] T. M. Hall, K. Nazarpour, and A. Jackson, "Real-time estimation and biofeedback of single-neuron firing rates using local field potentials," *Nature Commun.*, vol. 5, no. 1, p. 5462, Dec. 2014.

[31] J. R. Lackner and P. Dizio, "Rapid adaptation to coriolis force perturbations of arm trajectory," *J. Neurophysiol.*, vol. 72, no. 1, pp. 299–313, Jul. 1994.

[32] R. Shadmehr and F. Mussa-Ivaldi, "Adaptive representation of dynamics during learning of a motor task," *J. Neurosci.*, vol. 14, no. 5, pp. 3208–3224, May 1994.

[33] T. Brashers-Krug, R. Shadmehr, and E. Bizzi, "Consolidation in human motor memory," *Nature*, vol. 382, no. 6588, pp. 252–255, Jul. 1996.

[34] M. D. Serruya, N. G. Hatsopoulos, L. Paninski, M. R. Fellows, and J. P. Donoghue, "Instant neural control of a movement signal," *Nature*, vol. 416, no. 6877, pp. 141–142, Mar. 2002.

[35] L. R. Hochberg *et al.*, "Neuronal ensemble control of prosthetic devices by a human with tetraplegia," *Nature*, vol. 442, no. 7099, pp. 164–171, Jul. 2006.

[36] B. Jarosiewicz, S. M. Chase, G. W. Fraser, M. Velliste, R. E. Kass, and A. B. Schwartz, "Functional network reorganization during learning in a brain-computer interface paradigm," *Proc. Nat. Acad. Sci. USA*, vol. 105, no. 49, pp. 19486–19491, 2008.

[37] K. Ganguly, D. F. Dimitrov, J. D. Wallis, and J. M. Carmena, "Reversible large-scale modification of cortical networks during neuroprosthetic control," *Nature Neurosci.*, vol. 14, no. 5, pp. 662–667, May 2011.

[38] J. M. Carmena, "Advances in neuroprosthetic learning and control," *PLoS Biol.*, vol. 11, no. 5, pp. 1–4, May 2013.

[39] X. Zhou, R. N. Tien, S. Ravikumar, and S. M. Chase, "Distinct types of neural reorganization during long-term learning," *J. Neurophysiol.*, vol. 121, no. 4, pp. 1329–1341, Apr. 2019.

[40] P. J. Kyberd *et al.*, "MARCUS: A two degree of freedom hand prosthesis with hierarchical grip control," *IEEE Trans. Rehabil. Eng.*, vol. 3, no. 1, pp. 70–76, Mar. 1995.

[41] K. Lohse, N. Shirzad, A. Verster, N. Hodges, and H. Van de Loos, "Video games and rehabilitation: Using design principles to enhance engagement in physical therapy," *J. Neurologic Phys. Therapy*, vol. 37, no. 4, pp. 166–175, 2013.

[42] J. M. Hahne, M. Markovic, and D. Farina, "User adaptation in myoelectric man-machine interfaces," *Sci. Rep.*, vol. 7, no. 1, p. 4437, Dec. 2017.

[43] J. M. Hahne *et al.*, "Linear and nonlinear regression techniques for simultaneous and proportional myoelectric control," *IEEE Trans. Neural Syst. Rehabil. Eng.*, vol. 22, no. 2, pp. 269–279, Mar. 2014.

[44] J. M. Hahne, S. Dahne, H.-J. Hwang, K.-R. Müller, and L. C. Parra, "Concurrent adaptation of human and machine improves simultaneous and proportional myoelectric control," *IEEE Trans. Neural Syst. Rehabil. Eng.*, vol. 23, no. 4, pp. 618–627, Jul. 2015.

[45] J. M. Hahne, M. A. Schweisfurth, M. Koppe, and D. Farina, "Simultaneous control of multiple functions of bionic hand prostheses: Performance and robustness in end users," *Sci. Robot.*, vol. 3, no. 19, Jun. 2018, Art. no. eaat3630.

[46] M. B. Kristoffersen, A. W. Franzke, C. K. van der Sluis, A. Murgia, and R. M. Bongers, "The effect of feedback during training sessions on learning pattern-recognition-based prosthesis control," *IEEE Trans. Neural Syst. Rehabil. Eng.*, vol. 27, no. 10, pp. 2087–2096, Oct. 2019.

[47] M. Couraud, D. Cattaert, F. Paclet, P. Y. Oudeyer, and A. de Rugy, "Model and experiments to optimize co-adaptation in a simplified myoelectric control system," *J. Neural Eng.*, vol. 15, no. 2, Apr. 2018, Art. no. 026006.

[48] A. Heerschop, C. K. van der Sluis, E. Otten, and R. M. Bongers, "Performance among different types of myocontrolled tasks is not related," *Human Movement Sci.*, vol. 70, Apr. 2020, Art. no. 102592.

[49] R. Meijer and K. Nazarpour, "Prosthetics," U.S. Patent 20150374515 A1, Dec. 31, 2015. [Online]. Available: https://patents.google.com/patent/US20150374515A1

[50] G. C. Matrone, C. Cipriani, M. Carrozza, and G. Magenes, "Real-time myoelectric control of a multi-fingered hand prosthesis using principal components analysis," *J. NeuroEng. Rehabil.*, vol. 9, no. 1, p. 40, 2012.

[51] J. He, D. Zhang, N. Jiang, X. Sheng, D. Farina, and X. Zhu, "User adaptation in long-term, open-loop myoelectric training: Implications for EMG pattern recognition in prosthesis control," *J. Neural Eng.*, vol. 12, no. 4, Aug. 2015, Art. no. 046005.